

# **In-Situ Annealing of the (110) and (001) Surfaces of SrTiO<sub>3</sub> Nanocuboids by High-Resolution Transmission Electron Microscopy**

E. Liberti\*, A. I. Kirkland

Dr. E. Liberti, Prof. A. I. Kirkland  
Department of Materials  
University of Oxford  
16 Parks Road, Oxford OX1 3PH, United Kingdom  
emanuela.liberti@materials.ox.ac.uk

## **Abstract**

Thermal annealing of SrTiO<sub>3</sub> substrates is used in a wide range of applications, including films and nanoparticle growth, electronic devices, catalysis and photocatalysis. To predict and control reaction kinetics during high temperature treatments, it is essential to understand dynamics in real time. For this purpose, in-situ electron microscopy techniques are increasingly used, as structural changes can be monitored at the nanoscale. Herein, we report on the surface evolution of the (110) and (001) surfaces of SrTiO<sub>3</sub> nanocuboids observed in-situ during thermal treatment at 800 °C, using aberration corrected high-resolution transmission electron microscopy. By establishing a threshold for the cumulative electron dose, below which only temperature induced growth occurs, we observe the formation of epitaxial, faceted TiO islands, in agreement with previously reported results on the thermal treatment of (001) surfaces of SrTiO<sub>3</sub> in reducing environments. When surface evolution is a consequence of the combined effects of electron beam damage and temperature-induced growth, structural modification of the cuboids is highly dynamic. In this case formation of faceted islands occurs rapidly in conjunction with sublimation of the cuboids at considerably larger speeds than in the case of thermal treatment.

## **1. Introduction**

Thermal annealing treatments are routinely used in the synthesis of nanoparticles to tailor their size and shape. To control particle growth at elevated temperatures, understanding the dynamics of surface evolution is of primary importance. In this work we report on the thermal annealing of

SrTiO<sub>3</sub> (STO) nanocuboids, exhibiting highly ordered {110} and {001} facets. STO is an important material that can act as a substrate for the growth of high-temperature superconducting thin films<sup>[1-2]</sup> and plays a major role as a catalyst support<sup>[3]</sup> and in photocatalysis.<sup>[4]</sup> Understanding surface modifications of STO with temperature at the nanoscale is therefore extremely valuable to a wide range of industrial applications. To obtain in-situ structural information with atomic resolution at variable temperature, we have used in-situ heating aberration corrected High-Resolution Transmission Electron Microscopy (HRTEM).

In a recent HRTEM study, Lin Y. et al.<sup>[5]</sup> characterized the atomic surface structure of STO cuboids and showed that the surface terminations depend on the synthesis. The presence (or absence) of surfactant molecules at the surface, absorbed during synthesis, modifies the chemical environment of the facets, driving their structural relaxation. For example, in the presence of an oleic acid surfactant, the primary (001) exposed surface of the cuboids has a (1 x 1) SrO termination, whereas in acetic acid, the (001) and (110) surfaces of the cuboids are mostly TiO<sub>2</sub>-rich.<sup>[5-6]</sup> Several other examples of surface reconstructions have been observed on (annealed) SrTiO<sub>3</sub> single crystals, particularly for the (001) surface, depending on the preparation method. Studies of the annealing of substrates at high temperatures also exist in various oxidising and reducing conditions, including ultra-high vacuum (UHV).<sup>[7-10]</sup> However, the characterization of these annealed films has mostly been performed ex-situ, after thermal treatment. In-situ annealing HRTEM studies have also been reported for the (001) surface of SrTiO<sub>3</sub>, thermally treated at a temperature of 970 °C. However these results were obtained with an electron energy of 1.25 MeV.<sup>[11]</sup> Electron beam damage at high voltages can significantly differ from the mechanism that is generally encountered in intermediate voltage microscopes operating at typically 300 keV. To date, there have been no reported studies on the thermal annealing of STO at these voltages. Furthermore, there are no reports on the specific thermal treatment of cuboids, whose facets have specific (001) and (110) terminations. Finally, experimental procedures that differentiate between electron beam-induced and temperature-induced growths have not been explored for these systems.

## 2. Experimental

STO cubes were synthesised following as reported elsewhere.<sup>[5]</sup> The average size of the cuboids was approximately 20 nm, as reported by the authors.<sup>[5]</sup> Samples for TEM studies were prepared by dispersion in ethanol and drop casting onto a standard TEM grid coated with a holey carbon film and a SiN window-based heating chip for examination at room temperature and for annealing, respectively. A single tilt DENS heating holder was used for all in-situ experiments. HRTEM imaging was performed using a double aberration-corrected transmission electron microscope, equipped with an Schottky field emission gun, and operated at 200 keV [REF to OJ]. Aberrations were corrected using a Zemlin tableau [?REF] to achieve a phase constant region of 20 – 26 mrad (depending on the data set). After locating cuboids as close to the zone axis of interest, heating to 800 °C was initiated stepwise, without ramping (approximately 1 min per 200 °C step ). Focal series acquisition was carried out with a dwell time of 0.1 s, 0.2 s, 0.2 s per frame (depending on the data set) and a focal step of 1.6 nm. For exit wavefunction restoration a Wiener filter was used, as implemented in the Focal Tilt Series Restoration (FTSR) plug in.<sup>[12–14]</sup> Residual aberrations were corrected numerically using a real space phase plate. Image simulations were performed using the JEMS image simulation software based on the multislice method using linear imaging theory.<sup>[15–16]</sup>

## 3. Results and Discussion

To study structural modifications due to temperature only during annealing, we firstly investigated the effect of electron dose on the reconstructions of the facets. The intrinsic (110) surface of the cuboids is shown in Figure 1, for a nanoparticle oriented along the [110] zone axis. In this case, the (110) surface is not atomically flat, but step edges and kinks are observed along the [001] direction. These surfaces have TiO<sub>2</sub>-rich terminations, for example in the well-ordered (2 x 1) reconstruction of the (110) surface<sup>[10]</sup> as observed in the right hand side boxed region of Figure 1 a.

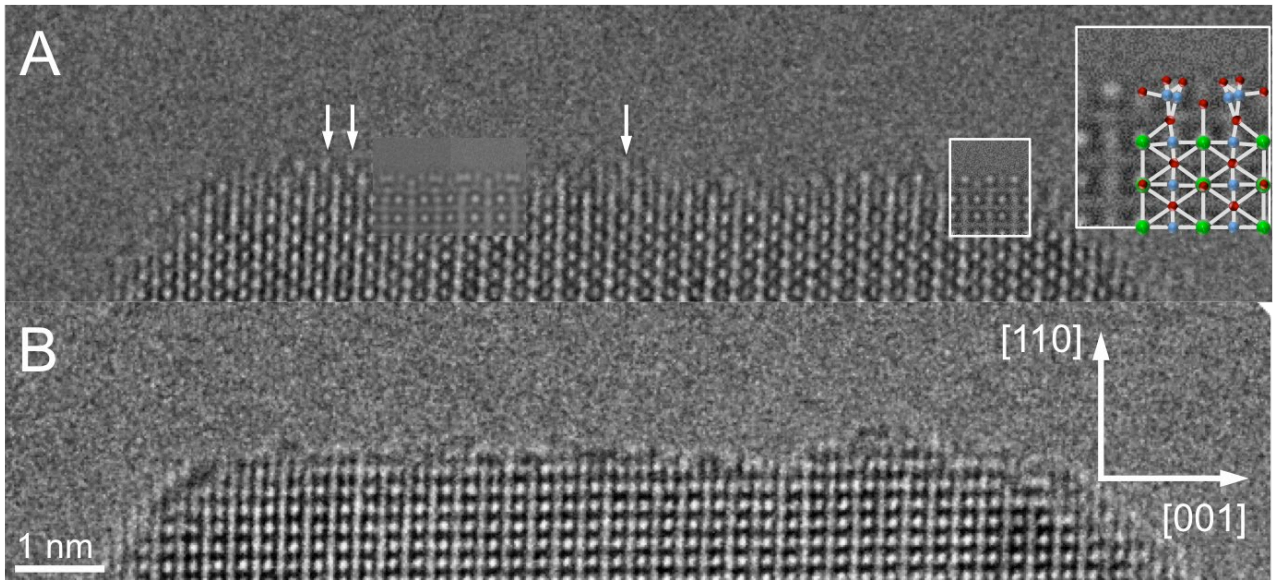


**Figure 1.** HRTEM images of a SrTiO<sub>3</sub> cuboid (110) surface, taken after 7 min (a) and 75 min (b) in a time-series of images, for a total cumulative electron dose of  $0.7 \times 10^{10} \text{ e}^-/\text{nm}^2$  (end of series). The inset in Figure (a), marked by the box, shows an image simulation of a (2 x 1) reconstruction, matching the experimental image for a defocus of -5 nm and thickness of 1.4 nm. Titanium, oxygen and strontium atoms in the atomic model are shown in blue, red and green, respectively. **Insets show simulated images for the (3 x 1) surface reconstruction at different thicknesses, which do not match the experiments.** For simulations values of  $C_3 = 2.3 \text{ } \mu\text{m}$  and  $C_5 = -1.8 \text{ mm}$  were used.

The rough surface structure along the [001] direction was generally observed for all cuboids, however the morphology changes between cubes, depending on the sample. This variation in roughness is provisionally ascribed to sample storage, synthesis and aging conditions. Additional layers of atoms, possibly TiO<sub>2</sub>-rich planes, were also observed stacking on the upper terraces of the (2 x 1) surface as indicated by the white arrows in Figure 1 (a). After imaging the (110) surface continuously in a time-series of HRTEM images for a cumulative electron dose of  $0.7 \times 10^{10} \text{ e}^-/\text{nm}^2$ , no significant structural rearrangement at the surface occurs. Although individual atoms were observed to hop between columns (Figures (a) and (b)), no overall phase change is observed under these imaging conditions (in Figure 1 (b) the surface is overfocused with respect to Figure 1 (a)). This cumulative dose can then be used as a threshold value above which electron-beam induced

effects start to dominate over temperature. At higher cumulative electron dose, the formation of new phases is observed.

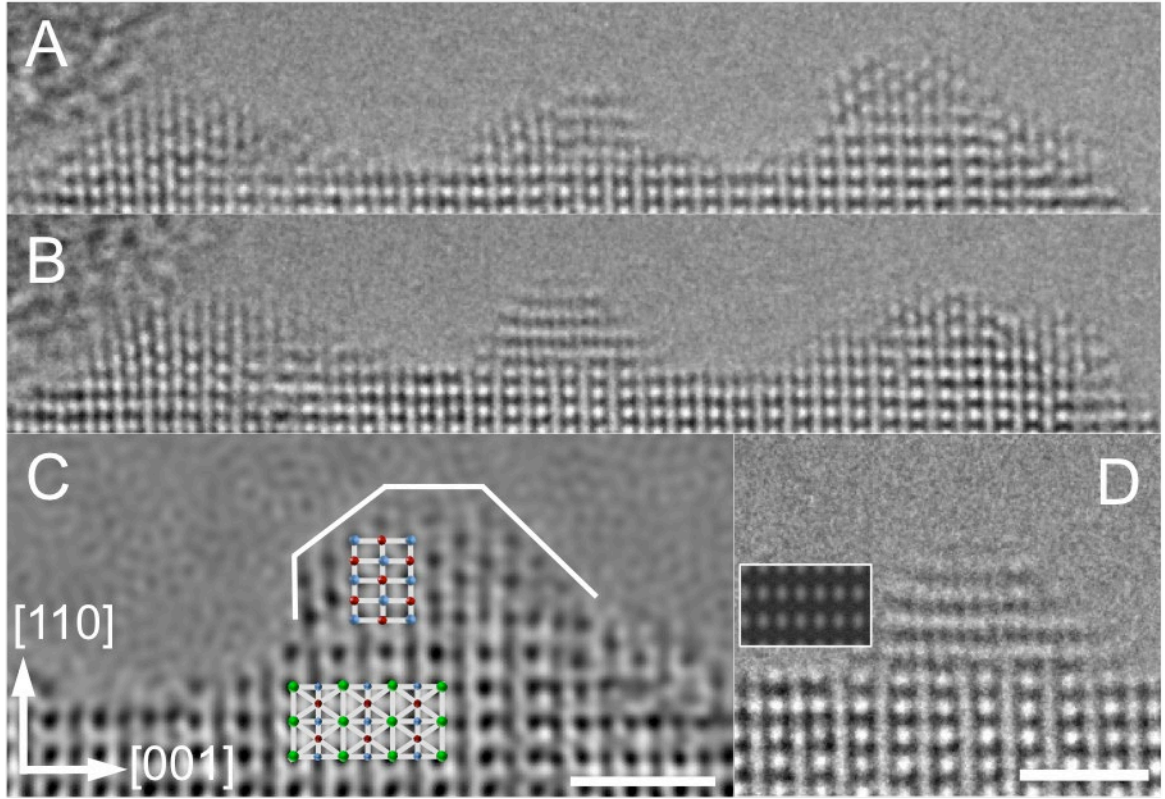


**Figure 2.** HRTEM images of a (110) cuboid surface under a cumulative electron dose of  $4.3 \times 10^{10} \text{ e}^-/\text{nm}^2$  (a) and  $7.6 \times 10^{10} \text{ e}^-/\text{nm}^2$  (b), corresponding to 55 min and 97 min of continuous imaging with a total dose of  $131 \times 10^5 \text{ e}^-/\text{nm}^2$ . Enlarged region of the restored phase (c) of the exit wavefunction corresponding to the cumulative dose in (a). 20 images of a focal series were used in the restoration. (c) Enlarged image of the middle island in (b), and corresponding image simulation (d). For the simulation,  $C_3 = 1.4 \text{ } \mu\text{m}$ ,  $C_5 = -861 \text{ } \mu\text{m}$ ,  $C_1 = -5 \text{ nm}$ , and a thickness of  $1.4 \text{ nm}$ , were used. Titanium, oxygen and strontium atoms are shown in blue, red and green, respectively.

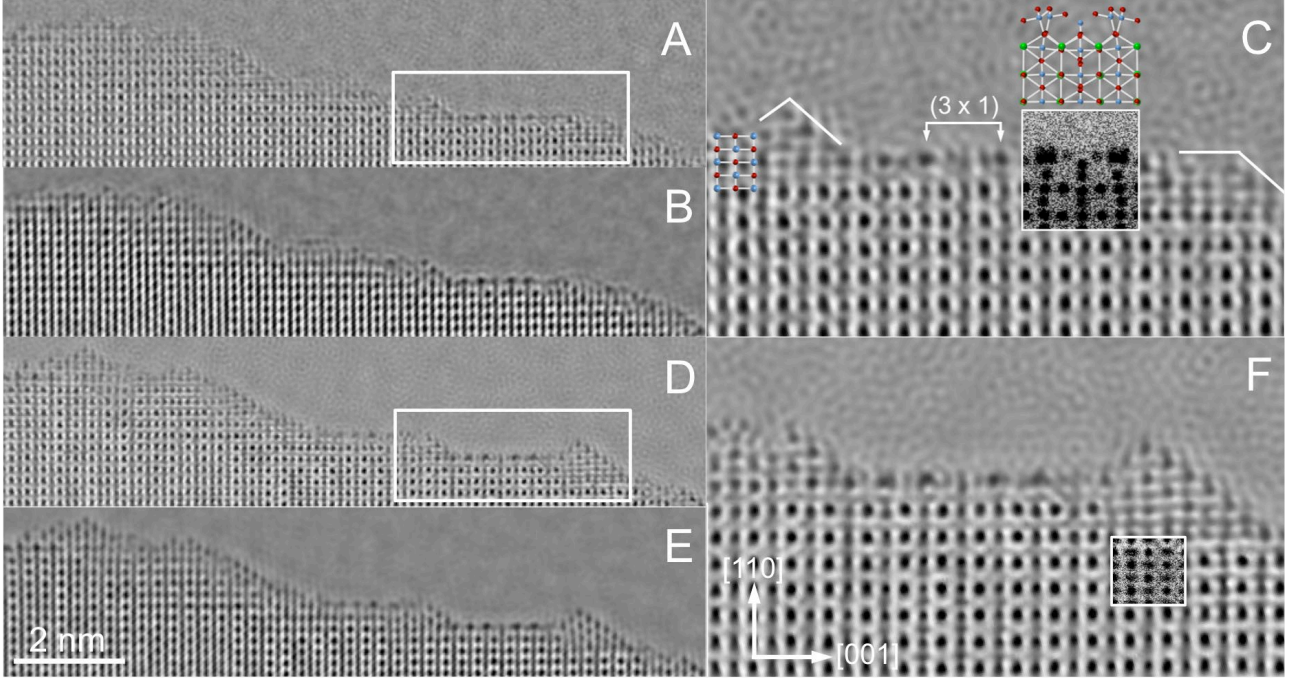
Figure 2 shows the formation of faceted islands on the (110) surface of a cuboid under a cumulative dose of  $4.3 \times 10^{10} \text{ e}^-/\text{nm}^2$  (a) and  $7.6 \times 10^{10} \text{ e}^-/\text{nm}^2$  (b).

Figure 2 (c) shows the phase of the exit wavefunction of the rightmost island in Figure 2 (a), restored at a cumulative electron dose of  $4.4 \times 10^{10} \text{ e}^-/\text{nm}^2$ . The lattice spacing along the [110] and [001] directions in the island were measured to be  $2.3 \text{ } \text{\AA}$  and  $3.2 \text{ } \text{\AA}$ , respectively, while variations

of 0.65 Å and 0.9 Å was found for the bulk, respectively. Taking these variations as the experimental error, the first set of values match closely the interplanar distances in the rocksalt TiO phase, at 2.9 Å and 4.2 Å for the (001) and (110) planes, respectively. Figure 2 (c) shows the phase shifts of both oxygen and titanium atoms columns present in the island and distinctive {001} and {111} surface facets. These facets are mostly terminated by titanium atoms columns on the (111) planes and by alternating Ti/O columns on the (001) planes. The interface between the (110) surface of the cuboid and the as-formed island is sharp and appears to be SrTiO terminated, suggesting a rearrangement of the initial (2 x 1) termination. As the accumulated dose increases, the TiO islands reshape, while the (110) surface of the cuboid sublimates. Lin et al.<sup>[17]</sup> have reported a similar behaviour for the reconstruction of the (001) surface of the cuboid, under a condensed electron beam. In this study, TiO and Ti metal surface islands are formed on a SrO terminated (001) surface of the cuboids, when the electron beam is focused onto the specimen for a few seconds (9 s). The formation of Ti metal islands is also observed as shown in Figure 2 (d). The measured lattice spacings in this case are 1.2 Å and 1.9 Å along the [110] and [001] directions respectively corresponding to bcc (Im-3m) metallic Ti.

Following annealing at a temperature of 800 °C, for a total cumulative dose of  $0.33 \times 10^{10} \text{ e}^-/\text{nm}^2$ , a similar behaviour for the reconstruction of the (110) surface induced by the electron beam is observed (Figure 3). However, as this cumulative dose is below the threshold value of  $0.7 \times 10^{10} \text{ e}^-/\text{nm}^2$  for the electron-beam induced growth, structural modifications observed in this case are attributed to temperature only.





**Figure 3.** Restored phase of the exit wavefunction of the (110) surface of a SrTiO<sub>3</sub> cuboid recovered from a focal series of 20 images ( $0.82 \times 10^8 \text{ e}^-/\text{nm}^2$ ) at the start of annealing at 800 °C (a) and after imaging for a cumulative dose of  $0.38 \times 10^8 \text{ e}^-/\text{nm}^2$  (d), for 188 min. (b) and (e) are masked with a high spatial frequency bandpass filter (cutoff frequency  $5.12 \text{ nm}^{-1}$ , corresponding to the (002) plane spacing). TiO-rich islands and inclined edges are clearly visible, including terraces having mixed (2 x 1) and (3 x 1) surface terminations (c). After heating at 800 °C with a cumulative electron dose of  $0.38 \times 10^{10} \text{ e}^-/\text{nm}^2$ , growth of TiO-rich islands is observed, with well-defined {001} and {111} facets, as shown in the restored phase of the exit wavefunction (f). For the simulation,  $C_3 = 111 \text{ nm}$ ,  $C_5$  of  $-5.8 \text{ mm}$ , and thickness of  $1.4 \text{ nm}$  were used.

In the above example, the native (110) surface of the cuboid is faceted, with alternating islands, terraces and inclined edges, as shown in Figures 3 (a) and (b). Terraces have mixed (2 x 1) and (3 x 1) terminations, while islands and edges are TiO<sub>2</sub>-rich (Figure 3 (c)). Following annealing for 188 min (corresponding to an accumulated dose of  $0.38 \times 10^{10} \text{ e}^-/\text{nm}^2$  in Figures 3 (c) and (d)), terraces and edges retain their atomic structure, while TiO islands, evolve into larger, faceted crystals, with {111} and {001} facets (the measured lattice spacings in Figure 3 (f) are  $2.4 \pm 0.6 \text{ \AA}$  and  $3.4 \pm 0.8$

Å along the [110] and [001] directions, matching closely the TiO rocksalt phase). This result is similar to the growth observed under only electron beam irradiation. However in this case, the growth rate is slower (approximately one unit cell per 168 min versus one unit cell per 55 min in the case of electron beam-induced growth). Lee et al.<sup>[11]</sup> have reported similar results for in-situ annealing of a SrTiO<sub>3</sub> (001) substrate at 970 °C, identifying the formation of TiO<sub>x</sub> crystalline islands (with  $0.8 \leq x \leq 1.25$ ) with well-defined {001} and {011} facets. In the case of annealing in the electron microscope, the sample is exposed to highly reducing conditions. According to Lee et al.<sup>[11]</sup> crystal growth under reducing atmospheres follows the point defect model of Moos and Härdtl<sup>[18–19]</sup> in which the atmosphere triggers the formation of oxygen vacancies at the surface. Following the enrichment of oxygen vacancies at the surface, strontium atoms migrate towards the bulk to maintain the Schottky equilibrium between strontium and oxygen for the point defects at a given temperature, leading to a higher concentration of titanium atoms at the surface. At high electron dose, the local increase in temperature induced by the electron beam is only a few degrees,<sup>[20]</sup> thus the enrichment of titanium at the surface cannot be ascribed to the temperature induced diffusion of oxygen vacancies. Hence we propose that the electron beam is responsible for the formation (and diffusion) of these vacancies according to the radiolytic Knotek-Feibelman mechanism.<sup>[21–23]</sup> In this case, the electron-specimen interaction results in the excitation of a core electron of the metal and the emission of Auger electrons from the oxygen. This emission leaves positively charged oxygen ions, which can subsequently be sputtered by the electron beam, leaving oxygen vacancies at the surface. When the effects of electron-beam induced growth and temperature-induced growth are combined (Figures 4 (a) – (f)), the reconstruction of the (110) surface of the cuboids is significantly faster. For example, for the island in Figure 4 (a), one unit cell grows in approximately 16 min, and sublimates in less than 35 min. In general under these conditions, the growth of the islands rapidly evolves, eventually leading to the formation of faceted TiO nanoparticles, whose shape approaches the Wulff shape for the anatase polymorph (Figures 4 (b), (d) and (f)).<sup>[24]</sup> Although the lattice parameters measured for the islands in Figure 4 are larger



than those measured in **previous cases** ( $3.3 \pm 0.4 \text{ \AA}$  and  $4.5 \pm 0.7 \text{ \AA}$  along the [110] and [001] directions, respectively), indicating a higher O/Ti ratio, they do not approach the interplanar distances in anatase. Overall, the effect of beam irradiation is to accelerate the gradient of the oxygen vacancy concentration leading to sublimation of the cuboid, which rapidly disappears and which in turns affects the growth rate of the TiO nanoparticles. In contrast to the case of annealing at 1.25 MeV, where the islands are stable over long times (6 h), in our work we have observed that the formation and disappearance of new phases rapidly changes. This highly dynamic behaviour is due to the different damage mechanisms. As observed by Lee et al.<sup>[11]</sup> the vacuum, also influences the rate at which surface reactions occur, affecting the stoichiometry of the islands.

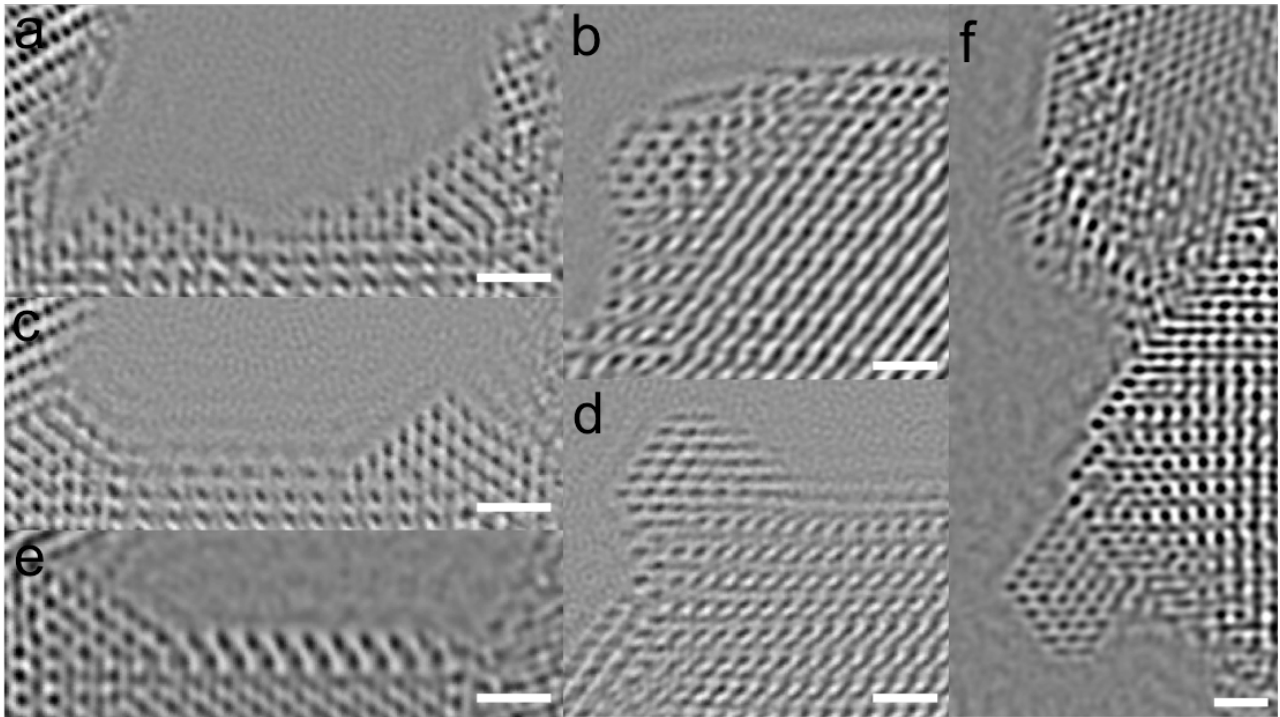


**Figure 4.** Reconstructed phases of the exit wavefunction of a [110] SrTiO<sub>3</sub> cuboid. Phases (a) and (b) correspond to adjacent (110) surfaces of the cuboid imaged at 500 °C, for a total cumulative dose of  $1.2 \times 10^{10} \text{ e}^-/\text{nm}^2$  (18 min with a total dose of  $109 \times 10^5 \text{ e}^-/\text{nm}^2$ ). The evolution of these facets is shown in (c), (d), (e) and (f), for total doses of  $3.6 \times 10^{10} \text{ e}^-/\text{nm}^2$  and  $4.7 \times 10^{10} \text{ e}^-/\text{nm}^2$ , at 800 °C, respectively (56 min and 72 min with a total dose of  $109 \times 10^5 \text{ e}^-/\text{nm}^2$ ). Scale bar in all figures is 1 nm.

The growth process of the islands is also affected by the presence of amorphous carbon at the surface. Similar to the observations of Lee et al.<sup>[11]</sup> when the substrate is coated with amorphous carbon, it is only after prolonged annealing that growth is observed. This is confirmed in Figure 5, which shows that the evolution of the (110) surface is considerably slower in the presence of carbon. Eventually, diffusion of carbon atoms occurs, leading to surface faceting (Figure 5 (c)).

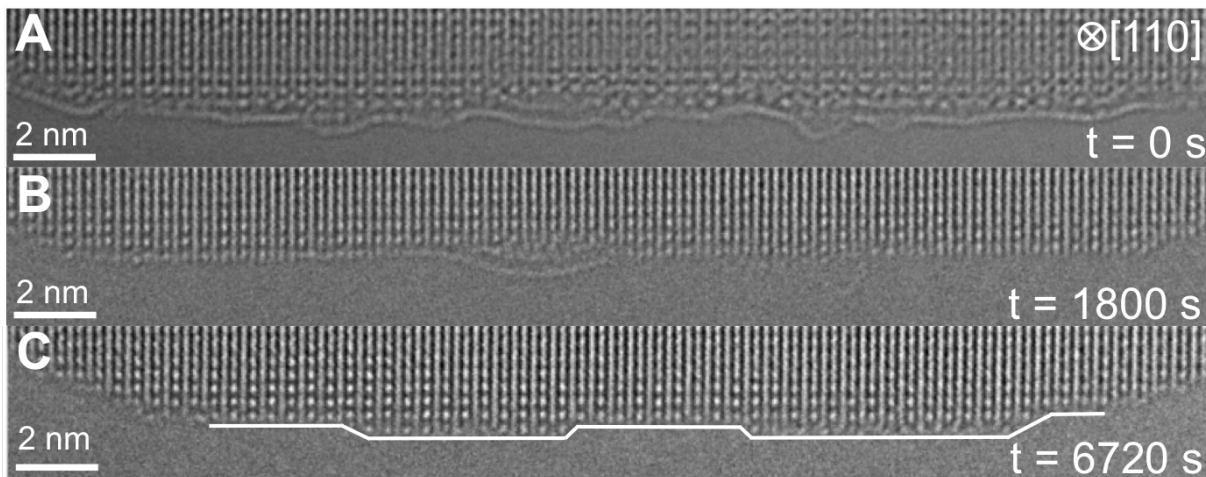


**Figure 5.** Time-series of HRTEM images illustrating the diffusion of hydrocarbons on the (110) surface of a STO cuboid at 800 °C.

In-situ annealing at 800 °C was also carried out to monitor the evolution of the (001) surface of the cuboids. An example is shown in Figure 6, for a cuboid aligned along a [001] zone axis. Consistent with the findings of Lin et al. (Lin, 2013) the {001} facet is SrO terminated, as expected for oleic acid synthesis. The adjacent (110) surface exhibits a SrTiO termination, as shown inset to Figure 1 (a), corresponding to the image simulation of a relaxed (6 x 1) termination, depleted of its TiO<sub>2</sub>-rich layer (also common to homologous (2 x 1), (3 x 1) and (4 x 1) terminations).<sup>[10]</sup> Following thermal treatment, the formation of faceted TiO<sub>x</sub> islands is observed on the (001) surface, in agreement with previous results.<sup>[11],[17]</sup> For the (110) surface, the reconstruction remains stable with temperature, before eventual sublimation.

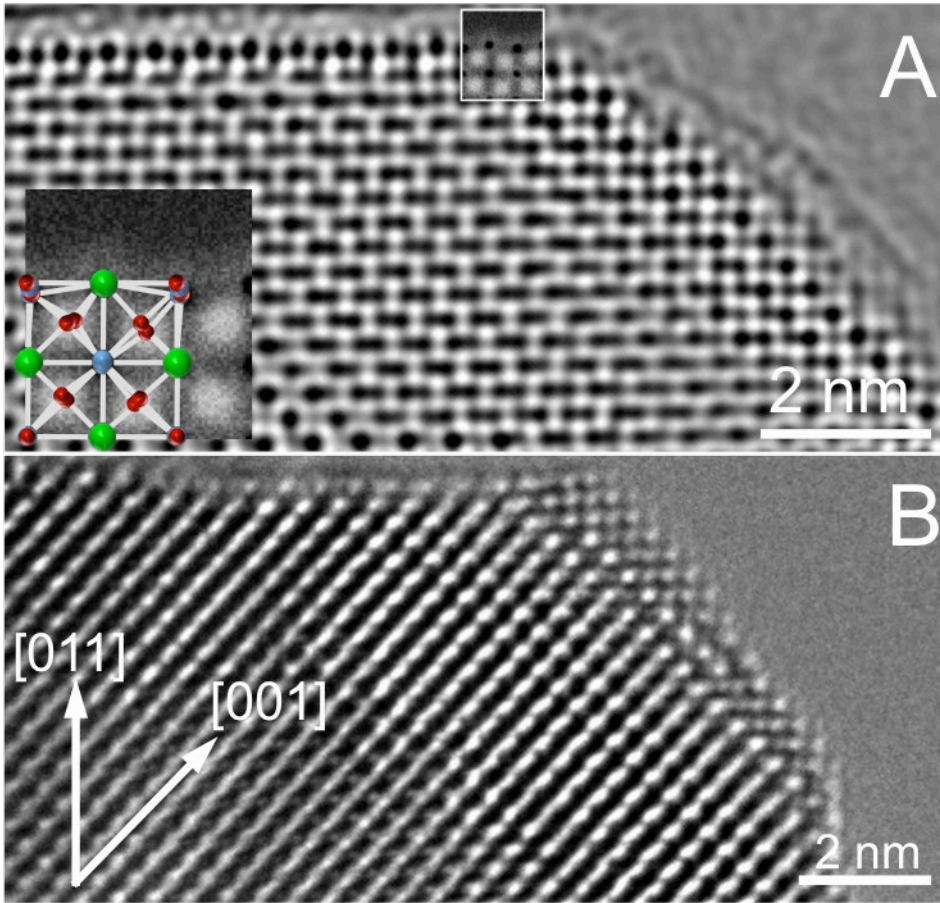


**Figure 6.** Restored phase of the exit wavefunction of an  $[001]$  oriented STO cuboid at room temperature (a). The  $(110)$  surface has a relaxed  $(6 \times 1)$  termination, depleted of its  $\text{TiO}_2$ -rich layer, in agreement with the simulation inset. For the simulation,  $C_2 = -582 \text{ nm}$ ,  $C_5 = 153 \text{ }\mu\text{m}$ , and a thickness of  $7 \text{ nm}$  were used. The  $(001)$  surface has a SrO termination. Following heat treatment at  $800 \text{ }^\circ\text{C}$ , the  $(001)$  surface forms TiO faceted islands, while the  $(110)$  surface sublimates, without structural rearrangement (b).

#### 4. Conclusions

In summary, we have studied the structural evolution of the  $(110)$  and  $(001)$  surfaces of  $\text{SrTiO}_3$  cuboids during thermal annealing at  $800 \text{ }^\circ\text{C}$ , using in-situ HRTEM. In agreement with previously reported studies on the electron beam damage of STO cuboids at  $200 \text{ keV}$  and in-situ HRTEM annealing at  $970 \text{ }^\circ\text{C}$  at  $1.25 \text{ MeV}$ , we have observe growth of epitaxial faceted TiO islands. By examining electron beam damage alone, we have established a threshold for the cumulative electron dose, below which temperature-induced growth only is observed. Thermal annealing under these

conditions results in the formation of faceted TiO islands as in the case of electron beam damage, however the growth rate in this case is considerably slower. Combining both effects, we have shown that surface restructuring is highly dynamic; the formation of TiO nanoparticles and sublimation of the cuboids occurring at greater speeds than in the case of individual electron beam and temperature-induced growths.

## Acknowledgments

The authors are grateful to Dr. Y. Lin, Prof. K. R. Poeppelmeier and Prof. L. D. Marks for providing the cuboids. The authors acknowledge the European Union under the Seventh Framework Programme under a contract for an Integrated Infrastructure Initiative Reference 312483-ESTEEM2. Financial support from EPSRC (Platform Grant EP/K032518/1) is also acknowledged. This manuscript is dedicated to the successful and exemplary career of Prof. J. Piqueras who was a mentor to the lead author.

## Conflict of Interest

The authors declare no conflict of interest

## Keywords

In-situ, annealing, HRTEM, SrTiO<sub>3</sub>

## References

- [1] Y. Sun, W. Zhang, Y. Xing, F. Li, Y. Zhao, Z. Xia, L. Wang, X. Ma, Q.-K. Xue, J. Wang, *Sci. Rep.* **2014**, *4*, 6040
- [2] D. Li, S. Gariglio, C. Cancellieri, A. Fête, D. Stornaiuolo, J.-M. Triscone, *APL Mater.* **2014**, *2*, 012102

- [3] X. Pan, L. Wang, F. Ling, Y. Li, D. Han, Q. Pang, L. Jia, *Int. J. Hydrogen Energy* **2015**, *40*, 1752
- [4] T. H. Chiang, H. Lyu, T. Hisatomi, Y. Goto, T. Takata, M. Katayama, T. Minegishi, K. Domen, *ACS Catal.* **2018**, *8*, 2782
- [5] Y. Lin, J. Wen, L. Hu, R. M. Kennedy, P. C. Stair, K. R. Poeppelmeier, L. D. Marks, *Phys. Rev. Lett.* **2013**, *111*, 156101.
- [6] L. A. Crosby, R. M. Kennedy, B.-R. Chen, J. Wen, K. R. Poeppelmeier, M. J. Bedzyk, L. D. Marks, *Nanoscale* **2016**, *8*, 16606.
- [7] J. Brunen, J. Zegenhagen, *Surf. Sci.* **1997**, *389*, 349.
- [8] M. R. Castell, *Surf. Sci.* 2002, **516**, 33.
- [9] B. C. Russell, M. R. Castell, *Phys. Rev. B* **2008**, *77*, 245414.
- [10] J. A. Enterkin, A. K. Subramanian, B. C. Russell, M. R. Castell, K. P. Poeppelmeier, L. D. Marks, *Nat. Mat.* **2010**, *9*, 245.
- [11] S. B. Lee, F. Phillipp, W. Sigle, M. Rühle, *Ultramicroscopy* **2005**, *104*, 30.
- [12] A. I. Kirkland, W. O. Saxton, K. L. Chau, K. Tsuno, M. Kawasaki, *Ultramicroscopy* **1995**, *57*, 355.
- [13] R. R. Meyer, A. I. Kirkland, W. O. Saxton, *Ultramicroscopy* **2002**, *92*, 89.
- [14] R. R. Meyer, A. I. Kirkland, W. O. Saxton, *Ultramicroscopy* **2004**, *99*, 115.
- [15] J. M. Cowley, A. F. Moodie, *Acta Cryst.* **1957**, *10*, 609.
- [16] P. Goodman, A. F. Moodie, *Acta Cryst. A* **1974**, *30*, 280.
- [17] Y. Lin, J. Wen, L. Hu, J. A. McCarthy, S. Wang, K. R. Poeppelmeier, L. D. Marks, *Micron* **2015**, *68*, 152.
- [18] R. Moos, K. H. Härdtl, *J. Am. Ceram. Soc.* **1997**, *80*, 2549.
- [19] W. Menesklou, H.-J. Schreiner, K. H. Härdtl, E. Ivers-Tiffée, *Sens. Actuators B: Chem.* **1999**, *59*, 184.
- [20] R. F. Egerton, P. Li, M. Malac, *Micron* **2004**, *35*, 399.

[21] P. J. Feibelman, M. L. Knotek, *Phys. Rev. B* **1978**, *18*, 6531.

[22] M. L. Knotek, P. J. Feibelman, *Phys. Rev. Lett.* **1978**, *40*, 964.

[23] M. L. Knotek, P. J. Feibelman, *Surf. Sci.* **1979**, *90*, 78.

(Barnard, 2005) A. S. Barnard, L. A. Curtiss, *Nano Lett.* **2005**, *5*, 1261.